Physics and Imaging in Radiation Oncology 35 (2025) 100793

Contents lists available at ScienceDirect

Physics and Imaging in Radiation Oncology

journal homepage: www.sciencedirect.com/journal/physics-and-imaging-in-radiation-oncology

Original research article

Tumour nuclear size heterogeneity as a biomarker for post-radiotherapy outcomes in gynecological malignancies

Yujing Zou [a,f,*,1], Harry Glickman [a,1], Manuela Pelmus [b], Farhad Maleki [c], Boris Bahoric [d], Magali Lecavalier-Barsoum [d], Shirin A. Enger [a,e,f]

[a] Medical Physics Unit, Department of Oncology, Faculty of Medicine, McGill University, Montreal, Canada
[b] Department of Pathology, Faculty of Medicine, McGill University, Montreal, Canada
[c] Department of Computer Science, University of Calgary, Calgary, Canada
[d] Department of Radiation Oncology, Jewish General Hospital, Montreal, Canada
[e] Lady Davis Institute for Medical Research, Montreal, Canada
[f] Montreal Institute for Learning Algorithms - Quebec AI Institute, Montreal, Canada

ARTICLE INFO

Keywords:
Radiotherapy
Tumour nuclear size
Biomarkers
Deep learning
Cox proportional hazards
Gynecological squamous cell carcinoma

ABSTRACT

Background and Purpose: Radiotherapy targets DNA in cancer cell nuclei. Radiation dose, however, is prescribed to a macroscopic target volume assuming uniform distribution, failing to consider microscopic variations in dose absorbed by individual nuclei. This study investigated a potential link between pre-treatment tumour nuclear size distributions and post-radiotherapy outcomes in gynecological squamous cell carcinoma (SCC).

Materials and Methods: Our multi-institutional cohort consisted of 191 non-metastatic gynecological SCC patients who had received radiotherapy with diagnostic whole slide images (WSIs) available. Tumour nuclear size distribution mean and standard deviation were extracted from WSIs using deep learning, and used to predict progression-free interval (PFI) and overall survival (OS) in multivariate Cox proportional hazards (CoxPH) analysis adjusted for age and clinical stage.

Results: Multivariate CoxPH analysis revealed that a larger nuclear size distribution mean results in more favorable outcomes for PFI (HR = 0.45, 95% CI: 0.19 - 1.09, p = 0.084) and OS (HR = 0.55, 95% CI: 0.24 - 1.25, p = 0.16), and that a larger nuclear size standard deviation results in less favorable outcomes for PFI (HR = 7.52, 95% CI: 1.43 - 39.52, p = 0.023) and OS (HR = 4.67, 95% CI: 0.96 - 22.57, p = 0.063). The bootstrap-validated C-statistic was 0.56 for PFI and 0.57 for OS.

Conclusion: Despite low accuracy, tumour nuclear size heterogeneity aided prognostication over standard clinical variables and was associated with outcomes following radiotherapy in gynecological SCC. This highlights the potential importance of personalized multiscale dosimetry and warrants further large-scale pan-cancer studies.

1. Introduction

Cervical cancer is an important global health challenge, especially in countries without access to robust screening and prevention programs [1]. Treatment decisions are largely based on the clinical staging system of the International Federation of Gynecology and Obstetrics [2]. Surgery is preferred for early-stage disease (stages IA to IB2), with radiotherapy used for patients with contraindications to surgery or high-risk pathologic factors, while concurrent chemoradiotherapy is the standard of care for patients with locally advanced disease (stages IB3 to IVA) [1,2]. Patients with distant metastases (stage IVB) are rare and have limited response to treatment [2]. The effectiveness of radiotherapy relies on multiple factors such as the cell cycle phase [3], repair capacity [4], hypoxia, genetic mutations [5,6], absorbed dose, and radiation quality [7]. Certain tumours demonstrate higher intrinsic radiosensitivity and favorable responses to radiation, whereas others exhibit increased resistance; for instance, Li et al. found that colorectal (HCT116) cells experience greater radiation-induced cell killing compared to more radioresistant prostate cancer cells (PC3) when exposed to photons of various energies [7].

* Correspondence to: 3755 Chem. de la Côte-Sainte-Catherine, Montréal, QC H3T 1E2, Canada
E-mail address: yujing.zou@mail.mcgill.ca (Y. Zou).
[1] Both authors contributed equally to this work.

https://doi.org/10.1016/j.phro.2025.100793
Received 29 January 2025; Received in revised form 30 May 2025; Accepted 4 June 2025
Available online 19 June 2025

Ionizing radiation primarily damages DNA in the nucleus. Absorbed dose is the mean of the stochastic distribution of energy deposited in a voxel. However, this averaged measure cannot fully capture the biological effects of ionizing radiation due to microdosimetric fluctuations in energy deposition at the cellular and subcellular levels. Specific energy is the microscopic equivalent of absorbed dose, the total energy imparted to a small volume, such as the cell nucleus, divided by its mass [8,9]. This parameter provides a more precise representation of radiation interactions at the cellular level, important for understanding variability in radiation-induced biological outcomes [10–12]. According to the target theory of Lea, the radiation dose is inversely related to target size [13]. Based on size, a nucleus may therefore receive no direct hits (i.e. underdosed) or conversely experience multiple ionizations within a few nanometers, generating complex clustered double-strand breaks [14–16]. Microdosimetric spread increases as target size decreases, meaning smaller nuclei display higher variance in energy deposition. Tumours with varying nuclear sizes might exhibit differing dose responses [17], modulating the overall efficacy of radiotherapy, an effect largely unaccounted for in standard treatment planning.

We hypothesized that there may be a link between nuclear size distribution (NSD) and clinical outcomes post-radiotherapy. While histological grading is used prognostically and for treatment planning in other cancers, grading has not historically been associated with treatment outcomes in cervical squamous cell carcinoma (SCC) [18–20]. Atkin et al. explored the role of nuclear diameter in cervical carcinoma and noted associations with post-radiotherapy patient outcomes [21–23]. However, those studies analyzed only small cell samples rather than modern digital histopathology whole-slide images (WSIs) and did not examine heterogeneity in NSD. To our knowledge, no large, systematic, digital pathology-based study has rigorously evaluated nuclear size heterogeneity as a radiotherapy prognostic biomarker in gynecological SCC. Here, we developed a methodological pipeline to automatically extract patient-specific NSDs from pre-treatment digital histopathology WSIs to investigate their potential link with post-radiotherapy progression and survival outcomes in a multi-institutional patient cohort. Gynecological malignancies were used as a proof of concept.

2. Materials and methods

2.1. Patient cohort selection and data collection

The study included gynecological SCC patients from Montreal's Jewish General Hospital (n = 45), and TCGA-CESC [24] (n = 146). We included all SCC cases that had diagnostic WSIs available, received confirmed or presumed radiotherapy, and did not have metastatic disease. Patients with locally advanced disease and for whom treatment type was not reported were presumed to have received radiotherapy. Stage IVB metastatic cases were excluded because the hypothesized link between nucleus size and outcomes under radiotherapy would not be expected to apply to metastatic disease; radiotherapy is generally not used with curative intent in Stage IVB [2]. A patient exclusion/inclusion flow diagram is included in Supplementary Figure S1. Of the 352 cases initially considered, 191 were included in the final analysis, including 42 progressions and 45 deaths.

2.2. Multivariable Cox Proportional Hazard outcome prediction model development: predictors, clinical endpoints, evaluation

We applied an events-per-candidate predictor parameter rule of thumb of 10–15 and determined that a maximum of four predictor parameters could be accommodated [25]. The following four predictors were selected: tumour NSD mean, tumour NSD standard deviation (SD), age at diagnosis, and clinical stage. Age and stage were selected a priori based on their ubiquitous use as clinical prognostic factors and their possible confounding effects due to potential associations with outcomes and nuclear features. HPV status has been used prognostically in recent literature [26,27], but was excluded from the main analysis due to limited sample size and a small proportion of HPV-negative cases. Operational outcomes such as complete resection or surgical debulking status would likely be strongly predictive, but were not available in our datasets. To minimize parameters, age was handled linearly, and clinical stage was dichotomized to early-stage disease (IA-IB2), and locally advanced cases (IB3-IVA) [2]. Two clinical outcomes were investigated: progression-free interval (PFI) and overall survival (OS). PFI and OS were measured from the date of diagnosis to the date of a new tumour event or death, respectively. Outcomes for the JGH cohort were retrieved according to approved REB guidelines and regulations, while those of the TCGA-CESC cohort [24] were obtained from Liu et al.'s integrated TCGA Pan-Cancer clinical data resource [28].

Missing data was handled by multiple imputation, using the *mice* package in R to impute 10 sets, with default settings [29]. Survival analysis using multivariate Cox proportional hazards (CoxPH) models was performed, with the same four predictors for PFI and OS. We considered uncorrected two-sided p-values of 0.05 significant and reported 95% confidence intervals (CI) of hazard ratio (HR). To correct for the inclusion of two outcome variables, we applied Bonferroni correction and lowered the significance threshold from 0.05 to 0.025. However, we did not strictly rely on this threshold to dichotomously interpret estimated p-values as statistically significant or not. Instead, we derived meaning using a combination of *p*-value and confidence interval as continuous measures, and effect size as indicated by the hazard ratio point estimate [30].

We estimated bootstrap-validated C-statistic, optimism, and graphical calibration curves using 1000 iterations and otherwise default settings using the *rms* R package. Post-hoc sensitivity analysis was performed examining alternate model specifications: univariate analysis, inclusion of HPV status, inclusion only of clinical parameters, inclusion only of NSD parameters, and inclusion of quadratic age, all using complete case analysis and calculating bootstrap-validated C-statistics. All statistical analyses were conducted in R version 4.4.1. Moreover, the REporting recommendations for tumour MARKer prognostic studies (REMARK) [31] and the transparent reporting of a multivariable prediction model for individual prognosis or diagnosis (TRIPOD) guidelines were followed [32].

2.3. Automatic extraction of biomarker: cancerous nuclear size distribution from diagnostic histopathology WSIs

The workflow for automatically extracting the cancerous NSD from a diagnostic H&E histopathology WSI is shown in Fig. 1. All WSIs for TCGA-CESC [24] were downloaded from the GDC Data Portal[2] filtered by .svs file format and Slide-Image [33]. They were semantically segmented using the pre-trained deep learning `fcn_resnet50_unet-bcss` model from the TIAToolbox library (version 1.5.1) [34] at 40x resolution with microns-per-pixel around 0.25. Tissue masks were automatically generated, eliminating the white background of each WSI. Subsequently, probability maps from all patches were automatically merged, producing continuous pixel-level tissue segmentation masks, including tissue classes of tumour, stroma, inflammatory, necrosis, and others.

Additionally, Hou *et al.*[35] publicly released expert-validated nuclei contours as polygon coordinates[3] for each TCGA-CESC [24] WSI. Each nucleus per patch was spatially aligned and mapped onto the corresponding tissue segmentation masks at a pixel-level correspondence. Each nucleus size was determined as the equivalent radius of the nucleus area in microns [36,37]. The automated semantic segmentation was visually quality-assured by a senior pathologist. The NSD statistics from the tumoural region of the entire histopathology WSI

[2] https://portal.gdc.cancer.gov/projects/TCGA-CESC.
[3] https://www.cancerimagingarchive.net/collection/tcga-cesc/.

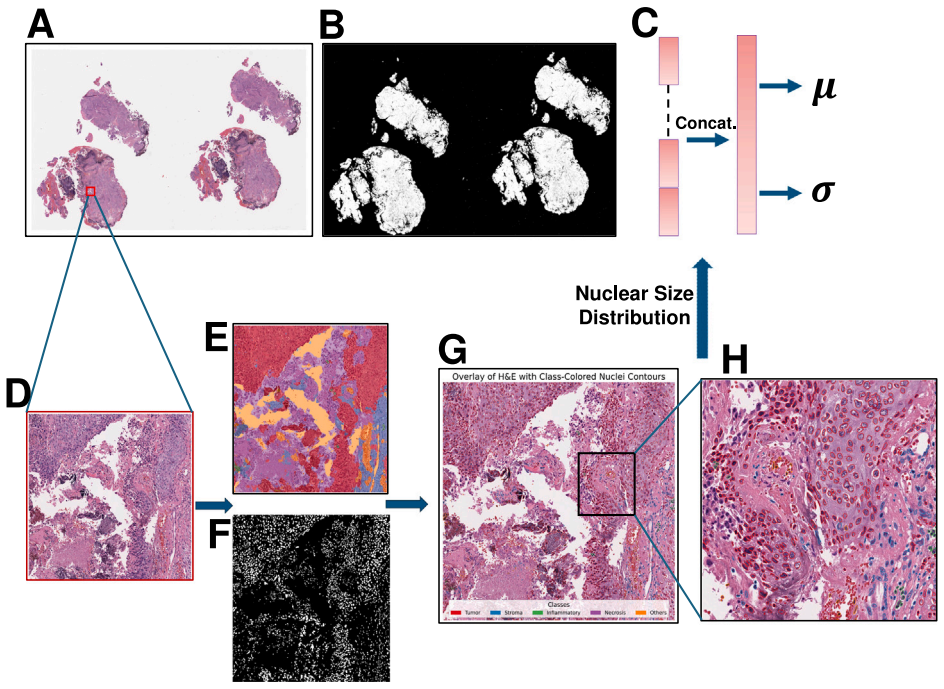

Fig. 1. Workflow to extract tumour nuclear size distribution (NSD) mean and SD from pre-treatment diagnostic H&E WSIs: (A) an example WSI at 40x resolution, (B) tissue masking of WSI; (C) tumour NSD from the entire WSI which were concatenated from each 4000 by 4000-pixel patch, resulting in tumour NSD mean and SD; (D) details of how the cancerous NSD was computed from a randomly selected patch: (E) semantic segmentation of the patch into five tissue classes (red: tumour, black: stroma, green: inflammatory, purple: narcosis, orange: others), (F) overlaying with the expert quality-assured nuclei segmentation; (G) tumour nuclei classified; (H) a zoomed-in patch of panel G.

per patient were used for the mean and SD calculation. After obtaining raw tumour NSDs for each WSI, histogram correction was applied to address potential image processing biases and artifacts, normalizing the distributions to represent nuclear radii accurately. Refer to supplemental materials for more implementation details and visualizations. Code for the image processing pipeline and statistical analyses were made publicly available on Github.[4]

3. Results

Patient characteristics, including NSD mean, NSD SD, age at diagnosis, clinical stage, HPV status, chemotherapy treatment, type of radiotherapy, total radiotherapy dose, and total number of fractions are presented in Table 1. HPV status, chemotherapy, and radiotherapy treatment information are included for comparison but were not included in the main model. Significance tests were performed separately for the two outcomes: two-sample t-tests for numeric variables and chi-squared tests of independence for categorical variables. HPV status was the only significant result in these univariate comparisons, with p-values of <0.005 for both outcomes. Furthermore, no collinearity or near-collinearity was observed in any of the predictors.

Unadjusted Kaplan–Meier curves for progression and survival in the first 5 years of follow-up, including censoring and number of events are included in Fig. 2. Patients were followed for approximately an average of 36 months, with a median follow-up of 25 and an interquartile range of 15 to 46 months.

Multivariate CoxPH estimates, 95% confidence intervals, and p-values are presented in Table 2. CoxPH analysis revealed a protective effect of NSD mean for PFI (HR = 0.45, 95% CI: 0.19–1.09,p = 0.084) and OS (HR = 0.55, 95% CI: 0.24–1.25,p = 0.16), and a harmful effect of NSD SD for PFI (HR = 7.52, 95% CI: 1.43–39.52,p = 0.023) and OS (HR = 4.67, 95% CI: 0.96–22.57,p = 0.063). Age and locally advanced disease results were non-significant, with HR near 1 for both PFI and OS. The bootstrap-validated C-statistic was 0.56 (optimism 0.05) for PFI and 0.57 (optimism 0.05) for OS, and graphical calibration showed an underestimation of early PFI and OS and an overestimation of late PFI and OS. Unadjusted Kaplan–Meier curves and associated log-rank tests for progression and survival according to nuclei size mean, and SD dichotomized at the median are presented in supplementary Figure S2.

Sensitivity analysis results are included in Table 3. Univariate analyses showed no significant results for the four main predictors. However, when HPV status was included as a predictor, positive HPV status had a significant protective effect for both PFI and OS, and NSD mean and SD were both near-significant for PFI (mean HR = 0.37, 95% CI: 0.14–0.99,p = 0.049, and SD HR = 6.46, 95% CI: 1.13–36.79,p = 0.036), but not for OS. When only clinical features were included, results were insignificant for age or clinical stage. When only NSD features were included, NSD SD was significant for PFI (HR = 7.15, 95% CI: 1.47 −34.7,p = 0.015) and near-significant for OS (HR = 5.23, 95% CI: 1.11–24.6,p = 0.036), but NSD mean was not significant for either, although the effect was still protective. When age was handled as a quadratic variable, the age terms became significant and NSD SD was significant for PFI (HR = 6.99, 95% CI: 1.33–36.65,p = 0.015). Bootstrap-validated C-statistics were also calculated for each model. Compared to the main analysis C-statistics of 0.56 for progression and 0.57 for survival, the inclusion of HPV status and quadratic age increased discrimination, univariate analyses and inclusion of clinical parameters decreased discrimination, and the use of only distribution parameters gave better discrimination for PFI and worse discrimination for OS.

4. Discussion

We retrospectively evaluated tumour nuclear size as a biomarker for radiotherapy outcomes from a multi-institutional cohort of gynecological cancer patients. We developed an automatic pipeline to derive patient-specific cancerous NSDs from gigapixel-sized H&E stained WSIs. Using multivariate CoxPH models, we estimated the effect of

[4] https://github.com/engerlab/segmentor.

Table 1
Summary of patient characteristics by progression and survival status. All patients received radiotherapy. HPV status, chemotherapy, and radiotherapy data were not included in the main analyses. Significance tests were performed separately for the two outcomes; two-sample t-tests for numeric variables and chi-squared tests of independence for categorical variables.

	No progression (N = 149)	Progression (N = 42)	Survived (N = 146)	Died (N = 45)	Overall (N = 191)
Nuclear Dist. Mean radius (μm)					
Mean (SD)	2.76 (0.435)	2.70 (0.555)	2.77 (0.447)	2.67 (0.509)	2.74 (0.463)
Nuclear Dist. Standard deviation (μm)					
Mean (SD)	1.25 (0.252)	1.29 (0.283)	1.26 (0.253)	1.27 (0.280)	1.26 (0.259)
Age at diagnosis					
Mean (SD)	51 (14)	53 (17)	51 (14)	54 (17)	52 (15)
Clinical stage					
Early stage	54 (36%)	18 (43%)	55 (38%)	17 (38%)	72 (38%)
Locally advanced	91 (61%)	24 (57%)	87 (60%)	28 (62%)	115 (60%)
Missing	4 (2.7%)	0 (0%)	4 (2.7%)	0 (0%)	4 (2.1%)
HPV status*					
Negative	4 (3%)	7 (17%)	4 (3%)	7 (16%)	11 (6%)
Positive	134 (90%)	33 (79%)	131 (90%)	36 (80%)	167 (87%)
Missing	11 (7.4%)	2 (4.8%)	11 (7.5%)	2 (4.4%)	13 (6.8%)
Chemotherapy (%)					
Mean (SD)	0.82 (0.39)	0.82 (0.39)	0.82 (0.39)	0.83 (0.38)	0.82 (0.39)
Missing	21 (14.1%)	4 (9.5%)	21 (14.4%)	4 (8.9%)	25 (13.1%)
Radiotherapy type					
Brachytherapy	2 (1%)	0 (0%)	2 (1%)	0 (1%)	2 (1%)
External beam radiotherapy	39 (26%)	13 (31%)	42 (29%)	10 (22%)	52 (27%)
Both	76 (51%)	24 (57%)	72 (49%)	28 (62%)	100 (52%)
Missing	32 (21.5%)	5 (11.9%)	30 (20.5%)	7 (15.6%)	37 (19.4%)
Total dose (Gy)					
Mean (SD)	66.9 (28.6)	67.0 (30.7)	67.1 (29.0)	66.4 (29.2)	67.0 (29.0)
Missing	39 (26.2%)	11 (26.2%)	35 (24.0%)	15 (33.3%)	50 (26.2%)
Total fractions					
Mean (SD)	30.8 (12.3)	30.4 (14.1)	31.1 (12.5)	29.1 (13.3)	30.7 (0.39)
Missing	53 (35.6%)	17 (40.5%)	51 (34.9%)	19 (42.2%)	70 (36.6%)

* Indicates HPV status was the only significant result in these univariate comparisons, with p-values of <0.005 for both outcomes.

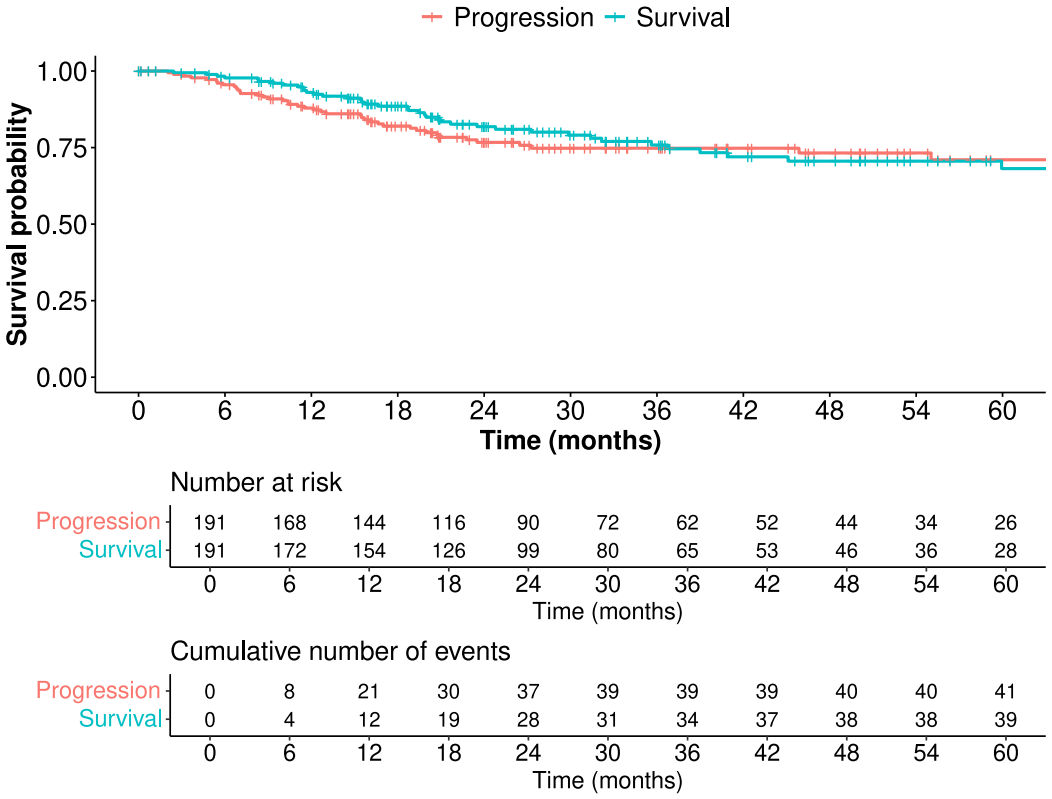

Fig. 2. Unadjusted Kaplan–Meier curves for progression and survival for the first 5 years of follow-up, including censoring and number of events.

pre-treatment NSDs on post-radiotherapy outcomes. Results demonstrated that a larger NSD mean was associated with improved PFI and OS, whereas a higher SD in NSD correlated with poorer outcomes. These findings suggest that nuclear size SD, or heterogeneity, could

Table 2
Multivariate Cox proportional hazards estimates, 95% confidence intervals, and p-values for progression free interval and overall survival.

Progression free interval CoxPH estimates				
Variable	Hazard Ratio	Lower 95% CI	Upper 95% CI	*p*-value
Nuclear Dist. Mean (μm)	0.45	0.19	1.09	0.084
Nuclear Dist. St. Dev. (μm)	7.52	1.43	39.52	0.023
Age	1.00	0.98	1.02	0.99
Locally advanced	0.88	0.47	1.63	0.68
Overall survival CoxPH estimates				
Variable	Hazard Ratio	Lower 95% CI	Upper 95% CI	*p*-value
Nuclear Dist. Mean (μm)	0.55	0.24	1.25	0.16
Nuclear Dist. St. Dev. (μm)	4.67	0.96	22.57	0.063
Age	1.00	0.98	1.03	0.70
Locally advanced	1.30	0.70	2.42	0.40

be a valuable prognostic biomarker in predicting the effectiveness of radiotherapy for gynecological malignancies.

CoxPH results revealed a protective though non-significant effect of increased NSD mean on post-radiotherapy outcomes, aligning with our hypothesis. With equal mean values of age, stage category, and NSD SD, patients with NSD means 1 μm greater would be expected to have approximately 0.45 times the rate of progressing, and 0.55 times the rate of dying at any given time-point. Conversely, results showed a harmful effect of increased NSD SD on post-radiotherapy outcomes. The effect was significant for PFI and non-significant for OS. With equal mean values of age, stage category, and NSD mean, patients with NSD SDs 1 μm greater would be expected to have approximately 7.52 times the rate of progressing and 4.67 times the rate of dying at any given time point. While results were not significant across all analyses, hazard ratio point estimates were large, indicating potentially clinically relevant effects.

One plausible explanation for these findings is that larger nuclei exhibit increased radiosensitivity. Differential NSDs across tumours may also relate to varying distributions of cell cycle stages, with correspondingly varying radiosensitivity [3,38–41]. The link between larger tumour nuclei and improved outcomes post-radiotherapy is concordant with previous work by Atkin et al. where gynecological SCC patients with larger, more DNA-rich nuclei had better long-term survival [21–23]. Furthermore, increased SD in NSD may indicate an increased presence of smaller nuclei which could escape lethal radiation damage due to an increased probability of fewer hits or no-hits in those nuclei [42,43]. Larger microdosimetric spread in the presence of small nuclei may contribute to a larger deviation between the specific energy imparted to nuclear targets and the prescribed macroscopic absorbed dose [9,11,42,43], leading to worse outcomes. Radiobiological modeling supports this observation. Wéra et al. demonstrated that larger NSD heterogeneity led to increased cell survival at high macroscopic doses, meaning that a fraction of cells, presumably those with smaller nuclei, survived even very high doses [12].

No significant effects were observed for age or locally advanced disease. Age was non-significant because of a U-shaped relationship, with younger (aged 20–39) and older (aged 70–89) having higher event rates, resulting in no linear trend. We presume the non-significance of locally advanced disease was due to the inclusion of only patients having received radiotherapy, which is given only to histologically aggressive cases of early-stage SCC or those with contraindications to surgery [2].

Sensitivity analysis of NSD estimates to alternate CoxPH model specifications was conducted: univariate analysis of the four main predictors, inclusion of HPV status as a predictor, inclusion of only clinical parameters, inclusion of only NSD parameters, and inclusion of age as a quadratic predictor. These alternate models explored the importance of multivariate analysis, a potential resolution of some degree of genetic confounding, the impact of clinical-only and nuclear-feature-only models, and better adjustment for the U-shaped relationship between age and outcome, respectively. Across these analyses, NSD SD was mostly a significant or near-significant predictor, and NSD mean remained near significance. Overall, these consistent trends supported our interpretations. Model discrimination was notably worse when nuclear features were not included, supporting the predictive power of these features. Also, the lack of significant trends in univariate analyses, and in dichotomized-at-the-median Kaplan Meier curves in Figure S2 was not surprising due to its lack of specificity and did not affect our interpretations.

Multivariate CoxPH discrimination reached a C-statistic of approximately 0.56 for PFI and 0.57 for OS, with bootstrap-estimated optimism of 0.05 for both, indicating some degree of overfitting. While absolute predictive performance was poor, including nuclear features did improve discrimination as compared to clinical features alone. Furthermore, these models were mostly intended to explore effect estimates and stimulate further study, not to be used directly for clinical predictions. The principal threat to the interpretation of results is likely confounding by genetics with more aggressive tumours potentially having larger nuclei [44,45]. Resolving this bias would likely increase the NSD mean estimate significance. Moreover, radiation quality differences may lead to variable relative biological effectiveness [7] and therefore clinical outcomes. Our patient cohort received primarily external beam radiation therapy (EBRT) or both brachytherapy and EBRT. However, it was infeasible to conduct radiation quality-specific analyses while adjusting for age and stage given our sample size. Larger cohorts would allow for estimation of nuclear feature effects stratified by radiation quality, as well as the inclusion of additional and more complex predictors. For example, one could explore the inclusion of additional stage categories, splined representation of age, and interaction terms between variables. Also, incorporating surgical outcomes might increase predictive power, if such data were available. However, surgical outcomes are unlikely to be strongly linked with pre-treatment nuclear features and thus should not have acted as confounding variables. There was also likely bias resulting from misclassification of tissue types. Based on pathologist visual quality assurance tumour nuclei were occasionally misclassified as stroma nuclei and necrotic areas near tumour regions were harder to distinguish. While imperfect, automatic segmentation was necessary to reduce manual labor and increase the speed of nuclear feature extraction.

Our findings suggest a potential link between pre-treatment tumour NSD parameters, particularly tumour nuclear size heterogeneity, and post-radiotherapy outcomes. This supported our hypothesis that tumour nuclear size influences radiosensitivity and clinical outcomes in gynecological SCC cancers. Larger nuclei may correlate with higher radiosensitivity, while heterogeneity in nuclear size may result in poorer outcomes due to underdosing smaller nuclei. Despite relatively poor predictive power, the inclusion of nuclear features also increased model discrimination compared to age at diagnosis and clinical stage. In the future, these findings should be validated through larger studies with diverse cancer types, including pan-cancer TCGA cohorts and prospective external validation by various institutions. Integrating nuclear morphology into personalized multiscale dosimetry bridges cellular response parameters like nuclear size heterogeneity with patient-level dosimetry. This requires fast and accurate patient-specific microdosimetry calculations to validate whether the prescribed absorbed dose reflects energy deposition at the subcellular level. Once validated with rigorous estimation of specific nuclear feature effects under different radiation qualities, clinical trials that adapt radiotherapy doses given a morphological marker could be conducted.

CRediT authorship contribution statement

Yujing Zou: Conceptualization, Data curation, Formal analysis, Investigation, Methodology, Software, Validation, Visualization, Writing

Table 3
Cox Proportional Hazards Model Estimates of Sensitivity Analyses for (a) Progression and (b) Survival. Univariate analysis, inclusion of HPV status, only including distribution parameters, and age as a quadratic variable were examined. Complete case analysis was performed. Bootstrap-validated C-statistics are presented for each model (C).

(a) Progression sensitivity analyses				
Variable	Hazard ratio	Lower 95% CI	Upper 95% CI	*p*-value
Univariate analysis: C 0.45, 0.54, 0.46, 0.46				
Nuclear mean (μm)	0.848	0.450	1.599	0.610
Nuclear SD (μm)	2.928	0.840	10.210	0.092
Age	1.007	0.985	1.028	0.539
Locally advanced	0.953	0.516	1.757	0.876
Inclusion of HPV status: C 0.57				
Nuclear mean (μm)	0.368	0.137	0.993	0.049
Nuclear SD (μm)	6.460	1.134	36.792	0.036
Age	0.997	0.974	1.021	0.820
Locally advanced	1.086	0.569	2.073	0.803
HPV positive	0.316	0.128	0.775	0.012
Only clinical parameters: C 0.43				
Age (μm)	1.006	0.985	1.028	0.561
Locally advanced (μm)	0.936	0.506	1.732	0.834
Only distribution parameters: C 0.58				
Nuclear mean (μm)	0.457	0.201	1.041	0.062
Nuclear SD (μm)	7.151	1.474	34.702	0.015
Quadratic age: C 0.59				
Nuclear mean (μm)	0.501	0.214	1.170	0.110
Nuclear SD (μm)	6.989	1.333	36.646	0.022
Age	0.848	0.741	0.970	0.016
Age^2	1.002	1.000	1.003	0.015
Locally advanced	0.890	0.479	1.655	0.713
(b) Survival sensitivity analyses				
Variable	Hazard ratio	Lower 95% CI	Upper 95% CI	*p*-value
Univariate analysis: C 0.46, 0.50, 0.48, 0.53				
Nuclear mean (μm)	0.840	0.457	1.542	0.573
Nuclear SD (μm)	2.356	0.700	7.931	0.166
Age	1.010	0.990	1.031	0.334
Locally advanced	1.361	0.741	2.500	0.321
Inclusion of HPV status: C 0.58				
Nuclear mean (μm)	0.434	0.170	1.110	0.081
Nuclear SD (μm)	4.395	0.824	23.446	0.083
Age	1.001	0.978	1.025	0.926
Locally advanced	1.582	0.840	2.980	0.156
HPV positive	0.276	0.112	0.680	0.005
Only clinical parameters: C 0.52				
Age (μm)	1.008	0.988	1.030	0.430
Locally advanced (μm)	1.331	0.751	0.723	0.359
Only distribution parameters: C 0.54				
Nuclear mean (μm)	0.503	0.228	1.110	0.089
Nuclear SD (μm)	5.233	1.111	24.640	0.036
Quadratic age: C 0.57				
Nuclear mean (μm)	0.581	0.265	1.273	0.175
Nuclear SD (μm)	4.759	0.978	23.159	0.053
Age	0.857	0.752	0.976	0.020
Age^2	1.002	1.000	1.003	0.016
Locally advanced	1.361	0.735	2.521	0.328

– review & editing. **Harry Glickman:** Conceptualization, Data curation, Formal analysis, Investigation, Methodology, Software, Validation, Visualization, Writing – review & editing. **Manuela Pelmus:** Data curation, Investigation, Methodology, Writing – review & editing. **Farhad Maleki:** Methodology, Visualization, Writing – review & editing. **Boris Bahoric:** Data curation. **Magali Lecavalier-Barsoum:** Conceptualization, Data curation, Formal analysis, Investigation, Methodology, Writing – review & editing. **Shirin A. Enger:** Conceptualization, Data curation, Formal analysis, Funding acquisition, Investigation, Methodology, Project administration, Resources, Supervision, Writing – review & editing.

Declaration of competing interest

The authors declare that they have no known competing financial interests or personal relationships that could have appeared to influence the work reported in this paper.

Acknowledgments

The authors acknowledge funding from the Canada Research Chairs Program (funding # 252135) and CHRP, Canada (NSERC+CIHR funding # 170620), TransMedTech Institute Excellence Scholarships and its primary funding partner, the Canada First Research Excellence Fund, the Fonds de recherche du Québec – Santé, Canada (FRQS funding # 319884), the Natural Sciences and Engineering Research Council of Canada-Canada Graduate Scholarships (NSERC-CGSD # 589759). The computing resources were partly enabled by support provided by Calcul Québec and the Digital Research Alliance of Canada, with immense staff expertise from Huizhong Lu. The results shown were also, in part, based upon data generated by the TCGA Research Network: http://cancergenome.nih.gov/. The authors also thank Joanna Li, Jonathan Kalinowski, Behnaz Behmand, and Mirta Dumancic for the fruitful discussions in this research.

Appendix A. Supplementary data

Supplementary material related to this article can be found online at https://doi.org/10.1016/j.phro.2025.100793.

References

[1] Cohen PA, Jhingran A, Oaknin A, Denny L. Cervical cancer. Lancet 2019;393:169–82. http://dx.doi.org/10.1016/S0140-6736(18)32470-X.

[2] Bhatla N, Aoki D, Sharma DN, Sankaranarayanan R. Cancer of the cervix uteri: 2021 update. IJGO 2021;155:28–44. http://dx.doi.org/10.1002/ijgo.13865.

[3] Pawlik TM, Keyomarsi K. Role of cell cycle in mediating sensitivity to radiotherapy. IJROBP 2004;59(4):928–42. http://dx.doi.org/10.1016/j.ijrobp.2004.03.005.

[4] Wieringa HW, van der Zee AGJ, de Vries EGE, van Vugt MATM. Breaking the DNA damage response to improve cervical cancer treatment. Cancer Treat Rev 2016;42:30–40. http://dx.doi.org/10.1016/j.ctrv.2015.11.008.

[5] Vaupel P, Harrison L. Tumor hypoxia: Causative factors, compensatory mechanisms, and cellular response. Oncologist 2004;9(S5):4–9. http://dx.doi.org/10.1634/theoncologist.9-90005-4.

[6] Seeber LMS, Horrée N, Vooijs MAGG, Heintz APM, van der Wall E, Verheijen RHM, et al. The role of hypoxia inducible factor-1alpha in gynecological cancer. Rev Oncol Hematol 2011;78(3):173–84. http://dx.doi.org/10.1016/j.critrevonc.2010.05.003.

[7] Li J, Chabaytah N, Babik J, Behmand B, Bekerat H, Connell T, et al. Relative biological effectiveness of clinically relevant photon energies for the survival of human colorectal, cervical, and prostate cancer cell lines. Phys Med Biol 2024;69(20):205008. http://dx.doi.org/10.1088/1361-6560/ad7d5a.

[8] Kellerer AM, Chmelevsky D. Concepts of microdosimetry II. probability distributions of the microdosimetric variables. Radiat Environ Biophys 1975;12(3):205–16. http://dx.doi.org/10.1007/BF01327348.

[9] Griffiths H. Microdosimetry. ICRU report no. 36. Radiology 1985;154(2). http://dx.doi.org/10.1148/radiology.154.2.528, 528–528.

[10] Gruel G, Villagrasa C, Voisin P, Clairand I, Benderitter M, Bottollier-Depois J-F, et al. Cell to cell variability of radiation-induced foci: Relation between observed damage and energy deposition. PLoS ONE 2016;11(1):e0145786. http://dx.doi.org/10.1371/journal.pone.0145786.

[11] Santa Cruz GA. Microdosimetry: Principles and applications. RPOR 2016;21(2):135–9. http://dx.doi.org/10.1016/j.rpor.2014.10.006.

[12] Wéra A-C, Barazzuol L, Jeynes JCG, Merchant MJ, Suzuki M, Kirkby KJ. Influence of the nucleus area distribution on the survival fraction after charged particles broad beam irradiation. Phys Med Biol 2014;59(15):4197. http://dx.doi.org/10.1088/0031-9155/59/15/4197.

[13] Lea DE. Actions of radiations on living cells. Radiology 1946;49(5):633–40. http://dx.doi.org/10.1148/49.5.633.

[14] Liu W, Tan Z, Zhang L, Champion C. Investigation on the correlation between energy deposition and clustered DNA damage induced by low-energy electrons. Radiat Environ Biophys 2018;57(2):179–87. http://dx.doi.org/10.1007/s00411-018-0730-0.

[15] Goodhead D. Initial events in the cellular effects of ionizing radiations: Clustered damage in DNA. Int J Radiat Biol 1994;65(1):7–17. http://dx.doi.org/10.1080/09553009414550021.

[16] Baiocco G, Bartzsch S, Conte V, Friedrich T, Jakob B, Tartas A, et al. A matter of space: how the spatial heterogeneity in energy deposition determines the biological outcome of radiation exposure. Radiat Environ Biophys 2022;61(4):545–59. http://dx.doi.org/10.1007/s00411-022-00989-z.

[17] Enger SA, Ahnesjö A, Verhaegen F, Beaulieu L. Dose to tissue medium or water cavities as surrogate for the dose to cell nuclei at brachytherapy photon energies. Phys Med Biol 2012;57(14):4489–500. http://dx.doi.org/10.1088/0031-9155/57/14/4489.

[18] Singh N, Arif S. Histopathologic parameters of prognosis in cervical cancer–a review. IJGC 2004;14(5):741–50. http://dx.doi.org/10.5005/jp/books/10109_2.

[19] Nunes TW, Filippi-Chiela EC, Callegari-Jacques SM, da Silva VD, Sansonowicz T, Lenz G, et al. Nuclear morphometric analysis in tissue as an objective tool with potential use to improve melanoma staging. Melanoma Res 2019;29(5):474–82. http://dx.doi.org/10.1097/CMR.0000000000000594.

[20] Carriaga MT, Henson DE. The histologic grading of cancer. Cancer 1995;75(S1):406–21. http://dx.doi.org/10.1002/1097-0142(19950101)75:1+<406::AID-CNCR2820751322>3.0.CO;2-W.

[21] Atkin NB, Richards BM. Clinical significance of ploidy in carcinoma of cervix: Its relation to prognosis. BMJ 1962;2(5317):1445–6. http://dx.doi.org/10.1136/bmj.2.5317.1445.

[22] Atkin NB. The chromosomal changes in malignancy; an assessment of their possible prognostic significance. Br J Radiol 1964;37(435):213–8. http://dx.doi.org/10.1259/0007-1285-37-435-213.

[23] Atkin NB. Carcinoma of the cervix: The influence of nuclear size and chromosome complement on prognosis of carcinoma of the cervix. J R Soc Med 1966;59(10):979–82. http://dx.doi.org/10.1177/003591576605901020.

[24] Lucchesi FR, Aredes ND. The cancer genome atlas stomach adenocarcinoma collection (TCGA-STAD). 2016, http://dx.doi.org/10.7937/K9/TCIA.2016.GDHL9KIM.

[25] Riley RD, Snell KI, Ensor J, Burke DL, Harrell Jr FE, Moons KG, et al. Minimum sample size for developing a multivariable prediction model: PART II-binary and time-to-event outcomes. Stat Med 2019;38(7):1276–96. http://dx.doi.org/10.1002/sim.7992.

[26] Li P, Tan Y, Zhu L-X, Zhou L-N, Zeng P, Liu Q, et al. Prognostic value of HPV DNA status in cervical cancer before treatment: a systematic review and meta-analysis. Oncotarget 2017;8(39):66352–9. http://dx.doi.org/10.18632/oncotarget.18558.

[27] Lei J, Arroyo-Mühr LS, Lagheden C, Eklund C, Nordqvist Kleppe S, Elfström M, et al. Human papillomavirus infection determines prognosis in cervical cancer. J Clin Oncol 2022;40(14):1522–8. http://dx.doi.org/10.1200/JCO.21.01930.

[28] Liu J, Lichtenberg T, Hoadley KA, Poisson LM, Lazar AJ, Cherniack AD, et al. An integrated TCGA pan-cancer clinical data resource to drive high-quality survival outcome analytics. Cell 2018;173(2):400–16. e11. http://dx.doi.org/10.1016/j.cell.2018.02.052.

[29] Van Buuren S, Groothuis-Oudshoorn K. Mice: Multivariate imputation by chained equations in r. J Stat Softw 2011;45:1–67. http://dx.doi.org/10.18637/jss.v045.i03.

[30] Greenland S, Senn SJ, Rothman KJ, Carlin JB, Poole C, Goodman SN, et al. Statistical tests, p values, confidence intervals, and power: a guide to misinterpretations. Eur J Epidemiol 2016;31(4):337–50. http://dx.doi.org/10.1007/s10654-016-0149-3.

[31] McShane LM, Altman DG, Sauerbrei W, Taube SE, Gion M, Clark GM. Reporting recommendations for tumour marker prognostic studies (REMARK). Br J Cancer 2005;93(4):387–91. http://dx.doi.org/10.1038/sj.bjc.6602678.

[32] Moons KG, Altman DG, Reitsma JB, Ioannidis JP, Macaskill P, Steyerberg EW, et al. Transparent reporting of a multivariable prediction model for individual prognosis or diagnosis (TRIPOD): explanation and elaboration. Ann Intern Med 2015;162(1):W1–73. http://dx.doi.org/10.1186/s12916-014-0241-z.

[33] Burk RD, Chen Z, Saller C, Tarvin K, Carvalho AL, Scapulatempo-Neto C, et al. Integrated genomic and molecular characterization of cervical cancer. Nature 2017;543(7645):378–84. http://dx.doi.org/10.1038/nature21386.

[34] Pocock J, Graham S, Vu QD, Jahanifar M, Deshpande S, Hadjigeorghiou G, et al. TIAToolbox as an end-to-end library for advanced tissue image analytics. Commun Med 2022;2(1):120. http://dx.doi.org/10.1038/s43856-022-00186-5.

[35] Hou L, Gupta R, Van Arnam JS, Zhang Y, Sivalenka K, Samaras D, et al. Dataset of segmented nuclei in hematoxylin and eosin stained histopathology images of ten cancer types. Sci Data 2020;7(1):185. http://dx.doi.org/10.1038/s41597-020-0528-1.

[36] DeCunha JM, Poole CM, Vallières M, Torres J, Camilleri-Broët S, Rayes RF, et al. Development of patient-specific 3D models from histopathological samples for applications in radiation therapy. Phys Medica 2021;81:162–9. http://dx.doi.org/10.1016/j.ejmp.2020.12.009.

[37] Poole CM, Ahnesjö A, Enger SA. Determination of subcellular compartment sizes for estimating dose variations in radiotherapy. Radiat Prot Dosim 2015;166(1–4):361–4. http://dx.doi.org/10.1093/rpd/ncv305.

[38] Yashar CM. 23 - basic principles in gynecologic radiotherapy. In: DiSaia PJ, Creasman WT, Mannel RS, McMeekin DS, Mutch DG, editors. Clinical gynecologic oncology (ninth edition). 2018, p. 586–605.e3. http://dx.doi.org/10.1016/B978-0-323-40067-1.00023-1.

[39] Dewey WC, Noel JS, Dettor CM. Changes in radiosensitivity and dispersion of chromatin during the cell cycle of synchronous Chinese hamster cells. Radiat Res 1972;52(2):373–94. http://dx.doi.org/10.2307/3573575.

[40] Maeshima K, Iino H, Hihara S, Imamoto N. Nuclear size, nuclear pore number and cell cycle. Nucleus 2011;2(2):113–8. http://dx.doi.org/10.4161/nucl.2.2.15446.

[41] Vignard J, Mirey G, Salles B. Ionizing-radiation induced DNA double-strand breaks: A direct and indirect lighting up. Radiother Oncol 2013;108(3):362–9. http://dx.doi.org/10.1016/j.radonc.2013.06.013.

[42] Villegas F, Tilly N, Ahnesjö A. Monte Carlo calculated microdosimetric spread for cell nucleus-sized targets exposed to brachytherapy ^{125} I and ^{192} ir sources and ^{60} co cell irradiation. Phys Med Biol 2013;58(17):6149–62. http://dx.doi.org/10.1088/0031-9155/58/17/6149.

[43] Villegas F, Tilly N, Ahnesjö A. Target size variation in microdosimetric distributions and its impact on the linear-quadratic parameterization of cell survival. Radiat Res 2018;190(5):504–12. http://dx.doi.org/10.1667/RR15089.1.

[44] Biswal BM, Othman NH. Correlation of nuclear morphometry and agnor score with radiation response in squamous cell cancers of the head and neck: A preliminary study. MJMS 2010;17(3):19–26.

[45] Baba AI, Câtoi C. Comparative oncology. Bucharest (RO): The Publishing House of the Romanian Academy; 2007.